Effect of Seasonal Changes for Identification of Disaster Areas with High Spatial Resolution Satellite Images

Toshiharu Kojima
River Basin Research Center, Gifu University
1-1 Yanagido, Gifu 501-1193, Japan
kojima@green.gifu-u.ac.jp

Kaoru Takara
Disaster Preventin Research Institute, Kyoto University
Gokasyo, Uji, Kyoto 611-0011, Japan
takara@mbox.kudpc.kyoto-u.ac.jp

Yasuto Tachikawa
Disaster Preventin Research Institute, Kyoto University
Gokasyo, Uji, Kyoto 611-0011, Japan
tachikawa@mbox.kudpc.kyoto-u.ac.jp

Abstract: The satellite images are expected to use for monitoring and identification of the disaster area. Subtraction of two images produces a differential image, which is useful to distinguish areas with surface condition change. In the case of identification of disaster areas the differential image is produced using images acquired before and after disaster in the area of interest. However the differential images have not been used efficiently due to some reasons. First reason is seasonal change of land surface properties between acquisition times of before- and after-disaster images. Second reason is spatial resolution of satellite images. Although middle spatial resolution satellites such as Landsat/TM and SPOT are used to distinguish larger-scale disasters such as flooding and forest fire, identification of small-scale disasters, such as landslide and collapsed buildings by earthquake, need higher spatial resolution than 10 m. In this paper, the authors proposed the new method to identify disaster areas with differential images modified seasonal changes and applied to the flood/landslide disaster areas, and investigate the effect of seasonal change and spatial resolution for identification of disaster areas using 4-m IKONOS images, 15-m ASTER/VNIR images, 30-m Landsat-7/ETM images and 1-km NOAA/AVHRR images. The new method has an instant effect on the identification of flood disaster areas at floodplain, but does not have much effect on landslide disaster areas. Seasonal land surface condition change between before- and after-disaster images does not so affect to the accuracy of landslide identification using high spatial resolution images, because landslide may occur inside of forest area, where landslide areas differ considerably from wood land irrespective of season in Japan. Compared to the ASTER image, IKONOS images improve the identification accuracies of 15 to 20 points. Although IKONOS images can identify the small disaster which covers an area of 10 m in width, ASTER image can not identify such a small landslide.
Keywords: IKONOS, high resolution interpolated image, linear mixture model, land surface change

1. Introduction

The satellite images are expected to use for monitoring and identification of the disaster area. Subtraction of two images produces a differential image, which is useful to distinguish areas with surface condition change. In the case of identification of disaster areas the differential image is produced using images acquired before and after disaster in the area of interest. However the differential images have not been used efficiently due to some reasons. First reason is seasonal change of land surface properties between acquisition times of before- and after -disaster images because of the following reasons:

1. Although high/middle resolution commercial satellites such as SPOT, Quick Bird and IKONOS can take some images after disaster by user requests, such satellites hardly ever take images before disaster because of no user request.
2. Landsat-7/ETM+ also can not take sufficient number of images due to some problems such as cloud and fixed data acquisition time interval.
3. Therefore, the acquisition times of before- and after-disaster images are often different, and it is difficult to distinguish only disaster areas due to effects of seasonal changes, which make confusion to distinguish disaster areas and other surface changes.

Second reason is spatial resolution of satellite images. Although middle spatial resolution satellites such as Landsat/TM and SPOT are used to distinguish larger-scale disasters such as flooding and forest fire, identification of small-scale disasters, such as landslide and collapsed buildings by earthquake, need higher spatial resolution than 10 m.

In this paper, the authors propose the new method to identify disaster areas with differential images modified seasonal changes and applied to the flood disaster areas in the Gamcheon river basin, South Korea. Moreover, the effect of seasonal change for identification of landslide areas is investigated using the 4-m IKONOS images and the 15-m ASTER/VNIR images in the Minamata River basin and the Yude River basin, Kyusyu, Japan, where the severe rainstorm hit and caused many landslides from July 19 to 21, 2003.

2. Method

1) Interpolation method with linear mixture model

Sensors with coarse spatial resolution such as NOAA/AVHRR (1.1 km) and MODIS (250-1000 m) can take images with higher temporal frequency. However, such coarse sensors do not have enough spatial resolution to investigate various disaster situations. On the other hand, higher spatial resolution sensors such as SPOT/HRV (10 – 20 m), IKONOS (1 – 4 m) and Landsat-7/ETM+ (15 – 30 m) can not take images with high temporal frequency. Note that some satellites have sensors of which observation angle can be changed. Such satellites enable to capture the disaster situations on successive days. We may use only a few images per year in a particular area of interest, in general. To overcome this disadvantage in satellite observation, the authors simulate the high resolution image that has the same radiometric properties as a coarse resolution image.

Puyou-Lascassies et al. [1] proposed the simulation of high resolution images, using a linear mixing model. Inamura [2] simulated high resolution thermal images from low resolution thermal band image and other high resolution band images of Landsat/TM using inverse matrix. In this study, the high resolution image is simulated as follows.

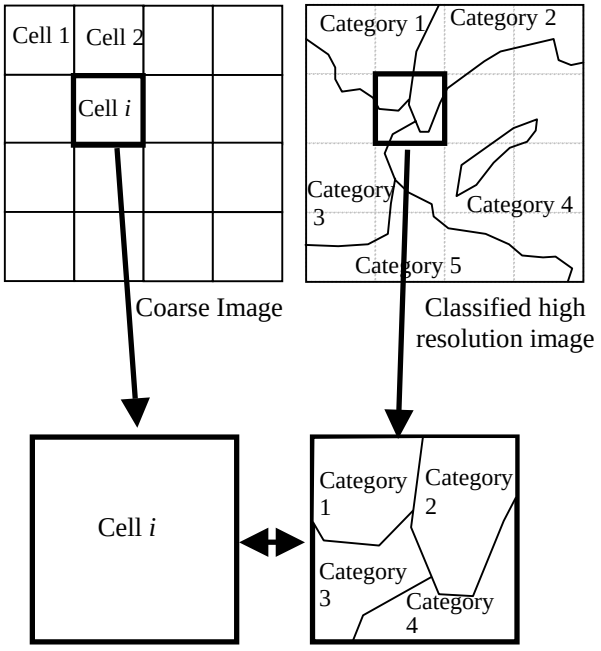

Fig. 1. Relationship each cell of the coarse resolution image and the classified high resolution image.

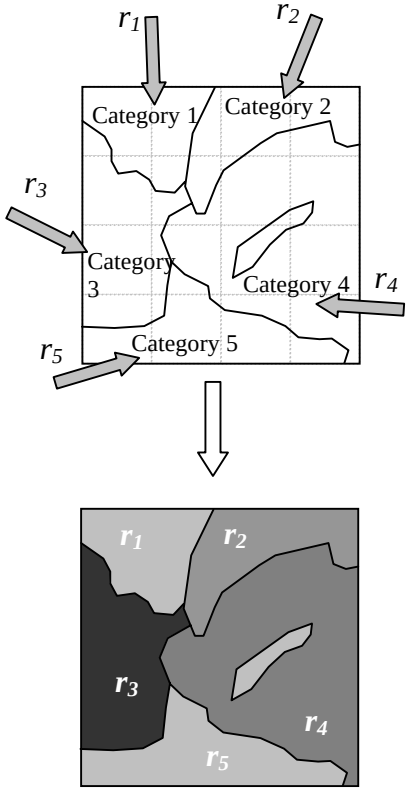

Fig. 2. Production of the interpolated image with the assigning the radiance of each category to each pixel of the classified high image.

1. A high resolution image can be classified into m land cover categories. Each pixel of a coarse resolution image includes several land cover categories in it.
2. Both of a coarse resolution image and a high resolution image are georeferenced to the same map coordinate system and the registration error between two images is very small.
3. A radiance of cell i in the coarse resolution image, R_i is explained the following equation using linear mixture model:

$$R_i = \frac{1}{A_i}\sum_{j}^{m} a_{ij} r_{ij} + e_i \qquad (1)$$

where, A_i is the area of cell i in the coarse resolution image, a_{ij} is the area of the j^{th} category in the cell i, r_{ij} is the radiance of the j^{th} category in the cell i and e_i is the error term (see Fig. 1).
4. The homogenous land cover has very little variability in the radiometric response. If we assume that the pixels of the j^{th} category have the same radiance over the whole zone, we can deduce that $r_{ij} = r_j$ in Eq. (1).

$$R_i = \frac{1}{A_i}\sum_{j}^{m} a_{ij} r_j + e_i \qquad (2)$$

where, r_j is the radiance of j^{th} category in the whole area. And we can estimate r_j with the multiple linear regression.
5. The higher resolution image can be simulated with assigning the values of r_j to each pixel of the classified high resolution image (see Fig. 2). The image is called the high resolution interpolated image (HRI image) here.

2) Differential images

The authors proposed the new method to produce a differential image using high and coarse resolution images. This method needs three images as follows:

1. A higher resolution image acquired after disaster (Image 1 in Fig. 3)
2. A higher resolution image acquired before disaster. This image may not be acquired in the same season as the after-disaster image (Image 2 in Fig. 3)
3. A coarser resolution image acquired before disaster. This image should be acquired in the same season as the after-disaster image or just before disaster (Image 3 in Fig. 3).

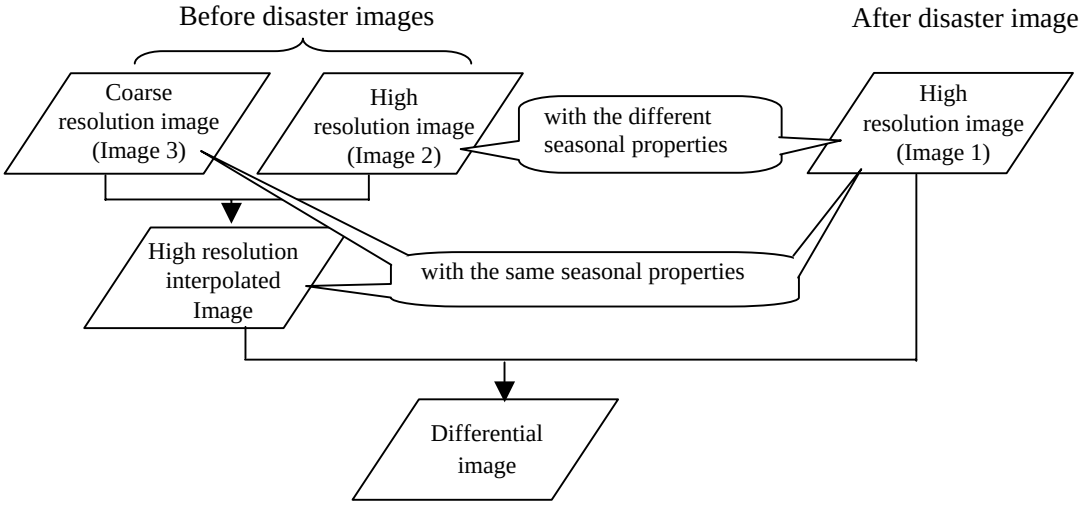

Fig. 3. Processing flow of the production of a differential image which is used for identification of disaster areas.

Usage of the image 1 and 2 is the traditional method to produce a differential image. However, there are seasonal differences between the image 1 and 2. So, the differential image is not proper for identification of disaster areas. Fig. 3 shows the processing flow of the new method. First, a high resolution interpolated image is simulated with a coarse resolution satellite image (Image 3 in Fig. 3) and a high resolution satellite image acquired before disaster (Image 2 in Fig. 3). A differential image is produced with the high resolution interpolated image and another high resolution image acquired after disaster (Image 1 in Fig.3). The differential image without the effect of seasonal change is used for identification of disaster areas.

3. Application to the flood disaster areas

1) Study area and satellite images

Typhoon Rusa swept through Korean Peninsula on August 31st and September 1st, 2002, and gave serious damage over the large area. The study area is the Gamcheon river basin, the middle part of South Korea where the 3-day rainfall (during August 30 to September 1) of 250 mm was recorded [3]. Typhoon Rusa caused much damage such as flooding, landslides and reservoir washouts.

Table 1 shows the list of satellite images used in this application. Landsat-7/ETM+ has 30-m spatial resolution and seven spectral bands as follows: Bands 1, 2 and 3 are visible region, Band 4 is near infrared, Bands 5 and 7 are middle infrared and Band 6 is thermal infrared. Repeat cycle of Landsat-7 is 17 days. NOAA/AVHRR has 1.1-km spatial resolution. NOAA satellites with AVHRR sensor can acquire several images per day.

Table 1. List of satellite images

Satellite / Sensor		Acquired Date	
Landsat-7/ETM$^+$	before flood	Nov. 19, 2001	(Image 2 in Fig.3)
	after flood	Sep. 3, 2002	(Image 1 in Fig.3)
NOAA/AVHRR	before flood	Sep. 16, 2001	(Image 3 in Fig.3)

2) Results and discussions

In this application, the differential images are produced with the NDVI images, because flood / landslide disaster have a tendency to vary the vegetation cover properties. Therefore, it is considered that differential NDVI image is effective to identify disaster areas. Note that the normal color composites can also give the same results.

Fig.4 shows the NDVI images produced with the Landsat-7 images acquired before/after disaster. Cultivated areas in the November image appear dark colored, for example the upper-left corner area in Fig. 4 (a). Because cultivated areas after harvesting have no crop and little vegetation such as stumps and straws, the areas have low vegetation activities and appear dark colored in the NDVI image. On the other hand, the cultivated areas in the September image appear light colored because of crops before harvesting (see Fig. 4 (b)). Urbanized areas appear dark colored due to little vegetation in all seasons.

Fig. 5 is the NDVI image produced with the NOAA/AVHRR image. Fig. 6 is the high resolution interpolated NDVI image, which has the same radiometric properties as the NOAA NDVI image acquired on September 16, 2001. The cultivated areas appear light colored in Fig. 6. This is almost the same as the Landsat-7 image acquired before harvesting (Fig. 4 (b)). The high resolution interpolated image can represent seasonal surface properties of the original coarse resolution image.

Fig. 7 shows the differential image obtained from the high resolution interpolated NDVI image and the after-disaster NDVI image. The ellipse at upper-left corner in Fig. 7 indicates flood disaster areas. The areas, which were originally cultivated area (paddy field), have been covered with sediments brought from upstream by the flood and indicated as white color. The disaster areas are clearly identified with the new identification method. Fig. 8 shows the differential image obtained by the conventional method that is simple subtraction of the before- and after-disaster images. The borders of flood areas around the main river stream are clearly shown in the both of Fig. 7 and 8. However, the flood disaster areas at the upper-left corner are not clearly identified, and there are many errors in the urbanized area. Consequently, the conventional method is not suitable to distinguish the flood disaster area, because of its seasonal error.

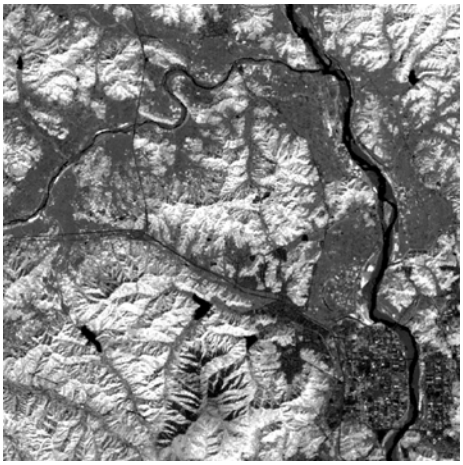

(a) before disaster (Nov. 19, 2001)

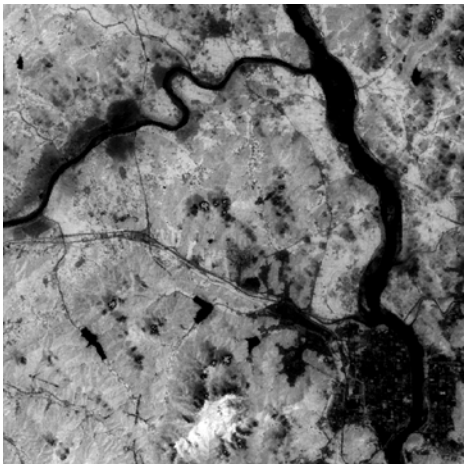

(b) after disaster (Sep. 3, 2002)

Fig. 4. The NDVI images with Landsat-7/ETM+ images at the Gamchon river basin.

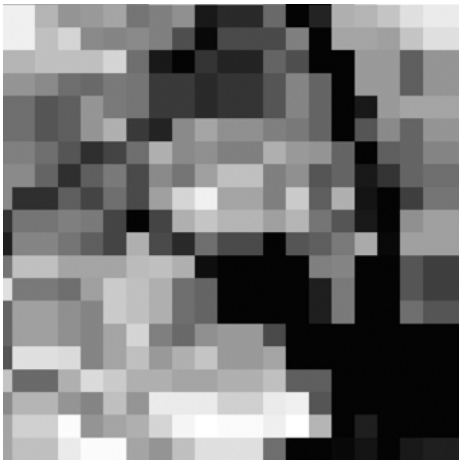

Fig. 5. NOAA NDVI image (Sep. 16, 2001).

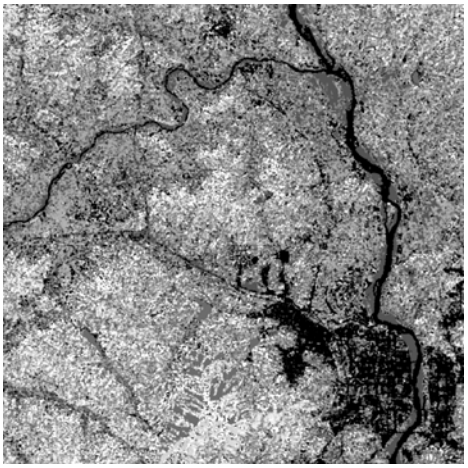

Fig 6. high resolution interpolated NDVI image, which has the same radiometric properties as the NOAA image (Sep. 16, 2001).

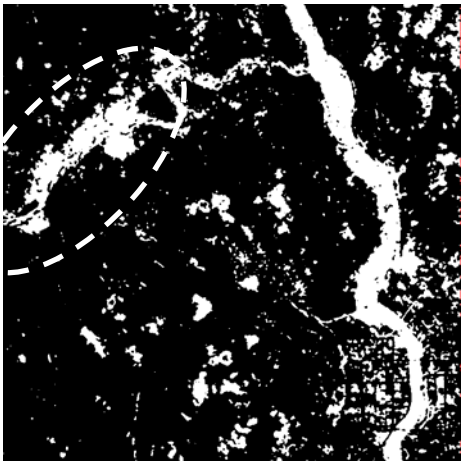

Fig. 7. Differential image with the new method

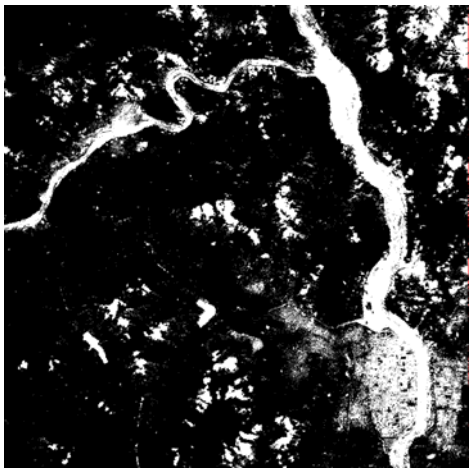

Fig. 8. Differential image with the conventional method.

4. Application to the landslide disaster areas

1) Study area and satellite images

The study area is the Minamata River basin and the Yude River basin, Kyusyu, Japan, where the severe rainstorm and the landslide disaster hit from July 19 to 21, 2003. Many landslides occurred in the river basin. Especially, large landslide at the Hougouchi,-Atumari area killed 15 persons. Also at the Arayashiki area, four persons died (see Fig. 9).

In this application, two 4-m IKONOS multispectral images and three 15-m Terra/ASTER VNIR images are used (Table 2). Two high resolution interpolated images (HRI images) are produced as follows (see Table 3):

HRI A: the IKONOS image acquired on Jul. 10, 2001 is used for the higher resolution image (Image 2 in Fig. 3) and the ASTER image acquired on Jul. 31, 2003 is used for the coarser resolution image (Image 3 in Fig. 3). This high resolution interpolated image has the summer surface condition which is the same as Jul. 31, 2003.

HRI A: the IKONOS image acquired on Jul. 10, 2001 is used for the higher resolution image (Image 2 in Fig. 3) and the ASTER image acquired on Feb. 15, 2004 is used for the coarser resolution image (Image 3 in Fig. 3). This high resolution interpolated image has the winter surface condition which is the same as Feb. 15, 2004.

The authors investigate the effects of seasonal changes and spatial resolution of satellite images using the following four image pairs:

Pair I: The HRI image A with almost the same seasonal properties as the after-disaster image is used for the before-disaster image. And IKONOS image acquired on Aug. 3, 2003 (just after disaster) is used for the after-disaster image. The seasonal change between the before- and after-disaster images is modified in this image pair.

Pair II: The HRI image B with winter surface condition is used for the before disaster image, and the IKONOS image acquired on Aug. 3, 2003 is used for the after-disaster image. This image pair includes the seasonal surface condition change between before- and after-disaster imagse.

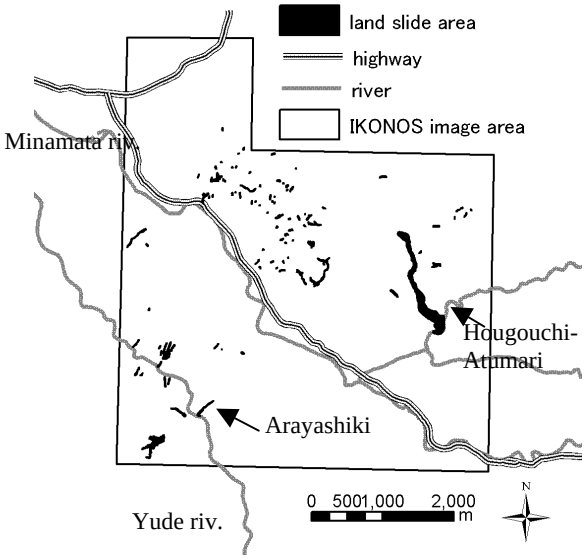

Fig. 9. The study area of the application to landslide disaster

Table 2 List of satellite images

Sat. Name			Obs. Date
IKONOS	Before Disaster		Jul. 10, 2001
	After Disaster		Aug. 3, 2003
ASTER	Before Disaster		Aug. 14, 2000
	After	Summer	Jul. 31, 2003
		Winter	Feb. 15, 2004

Table 3 Image pars of high resolution interpolated images are used for before-disaster images

	IKONOS	ASTER	
HRI A	Jul. 10, 2001	Jul. 31, 2003	With summer condition for image pairs I
HRI B	Jul. 10, 2001	Feb. 15, 2004	With winter condition for image pairs II

Pair III: IKONOS images are used for both of the before- and after-disaster images. This image pair does not include the seasonal surface condition change between before and after disaster images because the both of images were acquired at summer season (July and August).

Pair IV: ASTER/VNIR images are used. This image pair is used to confirm the effect of spatial resolution.

The differential images by simple subtraction are produced with the above image pairs. Ground truth image is obtained by visual photo-interpretation of the 1-m after-disaster IKONOS image which is resolution merged with the 1-m panchromatic image and the 4-m multispectral image. The landslide areas indicated in Fig. 9 are the ground truth data

with the merged IKONOS image. Identification accuracies of landslide areas are assessed with error matrix and user's accuracy (UA) and producer's accuracy (PA).

2) Results and discussions

Fig. 10 shows the landslide areas produced by the visual photo-interpretation using the after-disaster 1-m IKONOS image around the Arayashiki area. Fig. 11 to 14 show the differential image with the image pair I to IV, respectively. The pair I (Fig. 11) can distinguish the landslide areas except for the influence of the seasonal land surface condition changes between the before- and after-disaster images; meanwhile, the pair II (Fig. 12) is affected by the seasonal changes because the before-disaster image includes the land surface properties in winter. However, the landslide areas clearly appear black lines in the both figures. The pair III (Fig. 13) is the differential image using the original IKONOS images for before- and after-disaster images. All of the images of the pairs I to III are clearly indicate the landslide areas. The ASTER images also distinguish the landslide areas, however they does not appear so clearly.

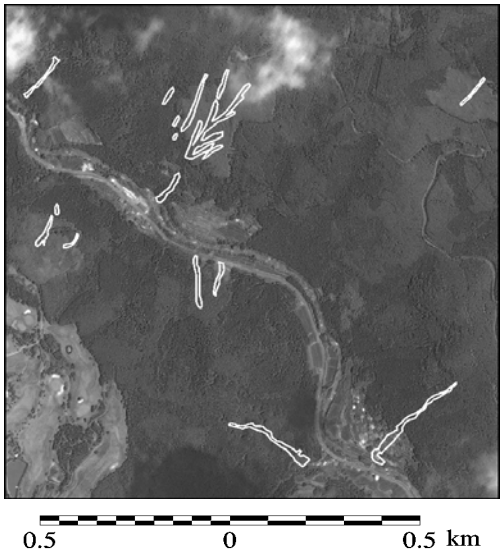

Fig. 10 Before-disaster IKONOS image and the landslide areas by aerial photo-interpretation at the Arayashiki area.

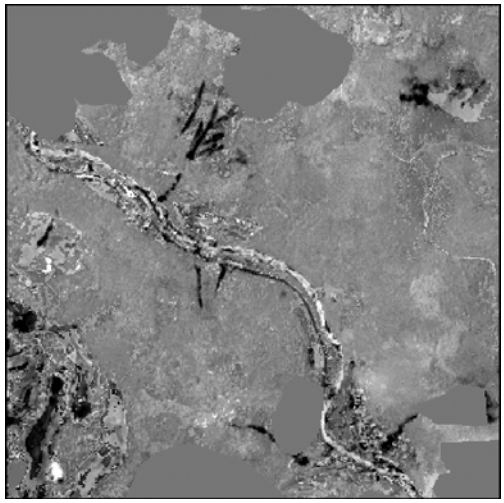

Fig. 11 Differential image with the image pair I. For the before disaster image, the modified image with the almost same land surface properties as the after disaster image was used.

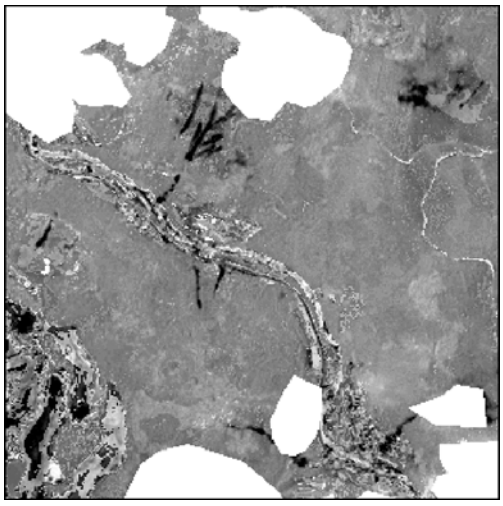

Fig. 12 Differential image with the image pair II. For the before disaster image, the modified image with the land surface properties of winter was used.

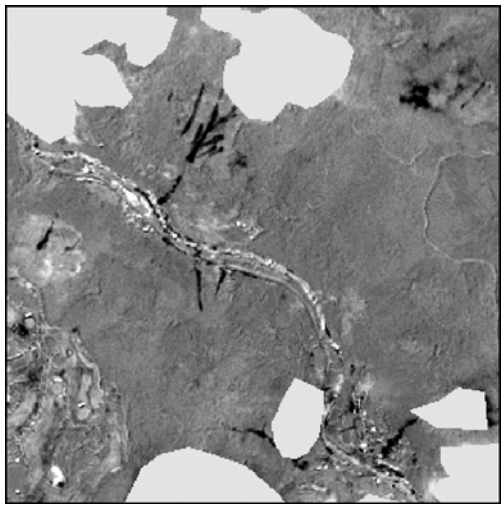

Fig. 13 Differential image with the image pair III. For the before disaster image, the IKONOS image acquired at July, 2001 was used.

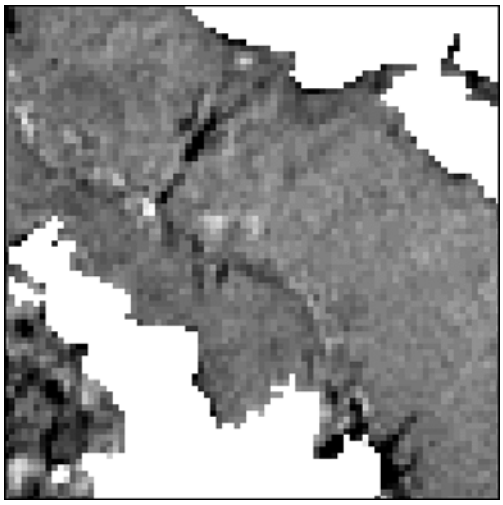

Fig. 14 Differential image with the image pair IV. Both of the before and after disaster images are the ASTER/VNIR images.

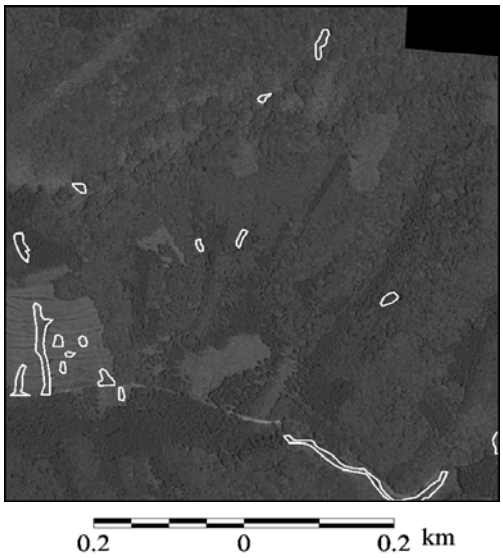

Fig.15 Before-disaster IKONOS image and land slide areas by aerial photo-interpretation at the Minamata river basin.

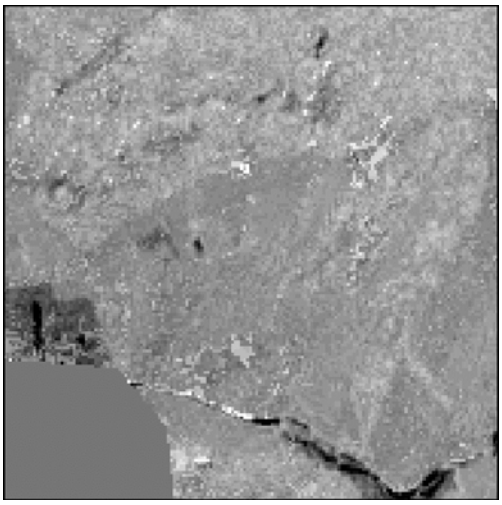

Fig.16 Differential image with the image pair I. For the before disaster image, the modified image with the almost same land surface properties as the after disaster image is used.

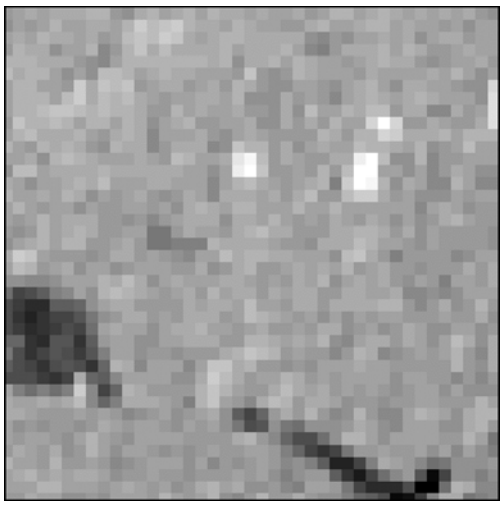

Fig. 17 Differential image with the ASTER images.

Table 3 Error matrix for the identification with the pair I

	Ground Truth			
Identified Data	Land Slide	Others	Total	UA
Land Slide	155852	345988	501840	31.1
Others	37826	14981646	15019472	
Total	193678	15327634		
PA	80.5%			

(Unit: m^2)

Table 4 Identification accuracies of each image pair

Pairs	PA	UA	Modified UA
I	80.5%	31.1%	39.7%
II	74.9%	36.6%	44.0%
III	74.1%	40.0%	48.7%
IV	61.5%	33.7%	-

Fig. 15 shows the landslide areas and before-disaster 1-m IKONOS image at the Minamata river basin. The landslides in this area are relatively small-scale. Almost of the landslides are less than 10 m in width. Fig.16 is the differential images with the pair I at the Minamata river basin. Fig. 17 is also the differential image with the ASTER images (the pair IV). Fig. 16 can distinguish some landslide areas. However, Fig. 17 can not find the landslide areas. 15-m ASTER image does not have the ability to extract the disaster areas of less than 10 m in width.

Table 3 is the error matrix for the identification of the landslide areas with the image pair I. PA is 80.5%, which indicates if we plan the field survey according to this identification result, we can survey more than 80% areas of the real disaster areas. Also 30% of UA indicates if we go to survey, 1/3 of areas would be real disaster areas. UA indicates relatively lower accuracy than PA. This reason can be explained as follows: some small landslide areas are overleaped in the ground truth data because of misinterpretation and urbanized areas was obviously no damaged by the landslide, however, urbanized areas were often assigned to landslide. The UA is modified by the exception of urbanize areas from the interesting area in order to reduce the error of UA. The modified UA of the pair I improves 31.1 to 39.7%.

Table 4 shows accuracies of identification with each image pair. Pairs I, II and III, which are produced with IKONOS images, show almost the same identification accuracies. Seasonal land surface condition change between before- and after-disaster images does not so affect to the accuracy of landslide identification using high spatial resolution images. very much. Because landslide may occur inside of the forest areas, landslide areas differ considerably from wood lands irrespective of season. Compared to the ASTER image, IKONOS images improve the identification accuracies of 15 to 20 points

5. Conclusions

Findings in this paper are summarized as follows:

1. Although the conventional differential image is a good method to extract surface changes, it is difficult to identify flood disaster areas because of seasonal surface change.
2. The authors proposed the new method using a high resolution interpolated image to identify flood disaster areas.
3. The new identification method with the high resolution interpolated image can exclude the effects of seasonal change and has a good capability to identify only flood disaster area without misinterpretation.
4. However, the new method does not have good efficiency to distinguish the landslide disaster areas at the mountainous areas, because almost mountainous areas are covered forest areas. The fluctuation of seasonal vegetation activities at the forest areas in Japan is very small, and it does not affect to identify the landslide areas. The landslide areas differ from wood lands irrespective of season. The landslide areas can identify without modification of seasonal change.
5. Although the 4-m IKONOS images can identify the small disaster which covers an area of 10 m in width, the 15-m ASTER image can not identify such a small landslide.

Acknowledgement

This research was supported by Grant-in-Aid for Integrated Sciences for Disaster Reduction in 2004, provided by the Kansai Research Foundation for technology promotion (KRF) of Japan.

References

[1] Puyou-Lascassies, Ph., A. Podaire and M. Gay, 1994. Extracting crop radiometric responses from simulated low and high spatial resolution satellite data using a linear mixing model, *International Journal of Remote Sensing*, 15(18): 3767-3784.

[2] Inamura, M., 1988. Improvement of Spatial Resolution for Low Spatial Resolution Thermal Infrared Image Using High Spatial Resolution Visible and Near-Infrared Images, *Journal of the Institute of Electronics, Information and Communication Engineers*, J71-A(2): 497-504 (in Japanese).

[3] Takara, K, 2003. Lessons from Disasters Brought by Typhoon RUSA, *Proceedings of Korea-Japan Joint Seminar on 2002 Flood Disaster by RUSA*, Korea Water Resources Corporation, August 2003, pp.3-5.